

PHASE-MATCHED FAR-INFRARED GENERATION  
BY OPTICAL MIXING OF DYE LASER BEAMS

K. H. Yang, J. R. Morris, P. L. Richards,  
and Y. R. Shen

RECEIVED  
LAWRENCE  
RADIATION LABORATORY

September 1973

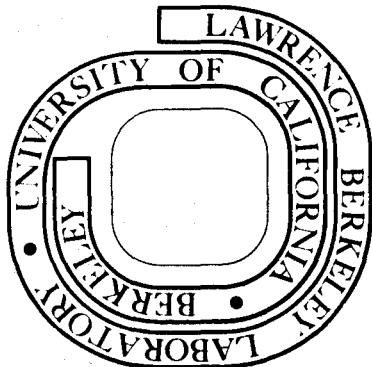
JAN 29 1974

LIBRARY AND  
DOCUMENTS SECTION

Prepared for the U. S. Atomic Energy Commission  
under Contract W-7405-ENG-48

**For Reference**

Not to be taken from this room



LBL-2226  
c.1

## **DISCLAIMER**

This document was prepared as an account of work sponsored by the United States Government. While this document is believed to contain correct information, neither the United States Government nor any agency thereof, nor the Regents of the University of California, nor any of their employees, makes any warranty, express or implied, or assumes any legal responsibility for the accuracy, completeness, or usefulness of any information, apparatus, product, or process disclosed, or represents that its use would not infringe privately owned rights. Reference herein to any specific commercial product, process, or service by its trade name, trademark, manufacturer, or otherwise, does not necessarily constitute or imply its endorsement, recommendation, or favoring by the United States Government or any agency thereof, or the Regents of the University of California. The views and opinions of authors expressed herein do not necessarily state or reflect those of the United States Government or any agency thereof or the Regents of the University of California.

Submitted to Applied Physics Letters

LBL-2226  
Preprint

UNIVERSITY OF CALIFORNIA

Lawrence Berkeley Laboratory  
Berkeley, California

AEC Contract No. W-7405-eng-48

PHASE-MATCHED FAR-INFRARED GENERATION BY OPTICAL MIXING OF  
DYE LASER BEAMS

K. H. Yang, J. R. Morris, P. L. Richards, and Y. R. Shen

SEPTEMBER 1973

Phase-Matched Far-Infrared Generation By Optical Mixing of  
Dye Laser Beams

K. H. Yang, J. R. Morris, P. L. Richards, and Y. R. Shen

Department of Physics, University of California,  
and

Inorganic Materials Research Division,  
Lawrence Berkeley Laboratory,  
Berkeley, California 94720

ABSTRACT

We report the use of a dual-frequency dye laser system to generate continuously tunable far-infrared radiation over the frequency range from 20 to  $190\text{ cm}^{-1}$ . We have investigated both collinear (forward and backward) and non-collinear phase-matching in  $\text{LiNbO}_3$  over most of this frequency range and forward collinear phase-matching in  $\text{ZnO}$ ,  $\text{ZnS}$ ,  $\text{CdS}$ , and  $\text{CdSe}$  at selected frequencies.

The generation of tunable far-infrared (FIR) by optical mixing in nonlinear crystals has attracted much attention recently.<sup>1-7</sup> In this Letter we report the generation of continuously tunable radiation from 20 to 190  $\text{cm}^{-1}$  using a dual-frequency dye laser system. We observed FIR radiation in the 20 to 160  $\text{cm}^{-1}$  frequency range with various phase matching schemes in  $\text{LiNbO}_3$ : forward collinear (FCPM), backward collinear (BCPM)<sup>3,4</sup> and non-collinear (NCPM). We have also investigated FCPM in ZnO, ZnS, CdS, and CdSe at selected frequencies as high as 190  $\text{cm}^{-1}$ . The observed FIR power is summarized in Table I.

Figure 1 shows the basic experimental arrangement for FIR generation with FCPM and BCPM. This single dye cell system was rather simple and very convenient to use. We also used two separate dye lasers<sup>8</sup> pumped with a single ruby beam, especially for the NCPM<sup>9</sup> case. The single dye cell system was composed of a single dye cell pumped nearly longitudinally by a ruby laser, a Glan-Thomson prism<sup>10</sup> (GTP) to divide the cavity into two independent arms with orthogonally polarized beams, two echelle gratings to tune independently the frequencies of the two beams, and a single output mirror to insure spatial overlap of the two beams. Temporal overlap of the beams was obtained by equalizing the net gain in the two arms of the cavity. To achieve this, the pump beam was circularly polarized or linearly polarized at  $45^\circ$  with respect to the axes of the polarizer. Fine tuning of the relative gain of the two arms was obtained with a microscope slide in the cavity. With a 30-MW, 30-nsec ruby laser beam the dye laser (DTTC iodide in DMSO) output had a peak power of 600 KW and its two wavelengths could be tuned independently from 8100 to 8400 Å. The linear polarizations were pure

to within 10%.

The FIR output from the non-linear crystal was collected by a brass light-pipe which was evacuated to avoid water vapor absorption. The FIR signal was detected by an n-type InSb (Putley) detector at 1.4K for the 20-95  $\text{cm}^{-1}$  range and a Ge:Ga detector at 4.2K for the 95-200  $\text{cm}^{-1}$  range. The sensitivity of the detector-amplifier system was measured by conventional Fourier transform spectroscopy using a calibrated Golay cell.<sup>8</sup> From this we could estimate the absolute FIR power. The wavelength of the FIR radiation was checked by a Fabry-Perot interferometer with metal mesh reflectors. We used the width of the phase matching peak at  $\omega_3 = 21 \text{ cm}^{-1}$  in a .16 cm-thick  $\text{LiNbO}_3$  crystal to measure the 3  $\text{cm}^{-1}$  <sup>11</sup> FIR bandwidth.<sup>8</sup>

In order to reduce statistical noise due to laser fluctuations, the FIR signal was normalized against the sum-frequency signal generated by reflection from a (110) surface of an InAs crystal,<sup>12</sup> which has a negligible dispersion over our frequency range. The intracavity microscope slide (see Fig. 1) that was used to adjust the relative gain of the two arms of the cavity was also used to couple out a fraction of the orthogonally polarized beams for the sum-frequency generation.

Our results on FCPM and NCPM in  $\text{LiNbO}_3$  are shown in Fig. 2. They can be explained by the following equation derived from the usual plane-wave approximation:

$$\frac{P_3}{P_1 P_2} = 16\pi^2 |\chi_{\text{eff}}^{(2)}|^2 \omega_3^2 n_3^2 T_1 T_2 T_3 / [c^3 |\tilde{n}_3|^2 n_1 n_2 (r_1^2 + r_2^2)] \quad (1)$$

$$* [1 - 2 \exp(-\alpha_3 \ell / 2) \cos(\Delta k \ell) + \exp(-\alpha_3 \ell)] / [(\Delta k)^2 + (\alpha_3 / 2)^2]$$

where  $P_i$  is the power ( $i = 1, 2$  for the input beams and  $i = 3$  for the FIR),  $k_i$  is the wavevector in the crystal,  $n_i$  is the refractive index,  $r_i$  is the beam radius at  $e^{-2}$  intensity,  $\alpha_3$  is the FIR absorption coefficient ( $\alpha_1 = \alpha_2 \approx 0$ ),  $T_1$  is the power transmission coefficient,  $\Delta k = |\vec{k}_1 - \vec{k}_2 - \vec{k}_3|$  is the phase mismatch,  $\ell$  is the crystal length or the effective length in the case of NCPM, and  $\chi_{\text{eff}}^{(2)}$  is the effective nonlinear susceptibility which depends on the crystal orientation. In calculating the theoretical curves in Fig. 2, we included the dispersion of  $n_3, \alpha_3$  (for the e-ray),  $T_3$ , and  $\chi_{\text{eff}}^{(2)}$ .<sup>13,14</sup> For the o-ray, we observed the values of  $\alpha_3$  by fitting the experimental phase matching curves in the FCPM case.<sup>15</sup>

The theoretical curves as shown in Fig. 2 describe the experimental data fairly well. In the FCPM results, ( $\chi_{\text{eff}}^{(2)} = \chi_{24}^{(2)} \sin\theta$ , where  $\theta$  is the angle between  $\vec{k}_1$  and the c-axis) the dip at  $65 \text{ cm}^{-1}$  is mainly due to the dispersion of  $\alpha_3$  which has an absorption peak around  $65 \text{ cm}^{-1}$  superimposed on the slope of the strong infrared mode at  $152 \text{ cm}^{-1}$ . We also observed backward propagating FIR radiation from  $20\text{--}95 \text{ cm}^{-1}$  generated using BCPM. In this case, the FIR was collected from the laser side of the crystal and a 1/8-inch hole was drilled in the collecting light pipe to allow the laser light to pass through. Due to the frequency dependent FIR loss through this hole and 5 cm of air in the collection path, these data were difficult to calibrate precisely. The BCPM power was estimated to be one to three times the FCPM signal throughout the  $40\text{--}95 \text{ cm}^{-1}$  frequency range, in rough agreement with Eq. (1), which predicts a factor of about 2.

In the NCPM case, a 4-mm cube of  $\text{LiNbO}_3$  was used with one corner cut off at  $68^\circ$  to let the generated FIR out (see the insert of Fig. 2).

The polarization of the two laser beams were both parallel to the c-axis and  $\chi_{\text{eff}}^{(2)} = \chi_{33}^{(2)}$ . Noncollinear phase-matching of FIR generation from 40-160  $\text{cm}^{-1}$  was achieved by varying angles  $\psi$  and  $\phi$  from  $0.81^\circ$  to  $9.18^\circ$  and from  $65.11^\circ$  to  $73.08^\circ$  respectively.<sup>14,16</sup> The FIR output in this case should be strongly affected by the divergence of the input beams. The theoretical curve for NCPM in Fig. 2 was therefore averaged over  $\Delta k$  from 0 to  $137 \text{ cm}^{-1}$ , which is appropriate for our 4 mrad beam divergence at the crystal. With  $\ell_{\text{eff}} = 0.5 \text{ mm}$ , it fits the experimental data very well. The steady decrease in the FIR signal with  $\omega_3$  above  $55 \text{ cm}^{-1}$  (where  $\alpha_3 \ell_{\text{eff}} \gg 1$  and  $\ell_{\text{eff}}$  is not an important parameter) is due to the increasing e-ray absorption.<sup>14</sup> The decrease on the low frequency side is due to the laser beam divergence and the  $\omega_3^2$  radiation efficiency factor.

Compared with the FCPM scheme, the NCPM scheme requires only one crystal for operation over a wide frequency range but needs two angular adjustments to orient the crystal for phase-matching. It generates more FIR power (Fig. 2) than the FCPM scheme for two basic reasons. First, since  $\chi_{33}^{(2)} \cong \chi_{24}^{(2)}$ ,<sup>17</sup>  $\chi_{\text{eff}}^{(2)}$  for FCPM is reduced by a factor of  $\sin\theta$ , which decreases at low frequencies. Second, the FIR e-ray generated with NCPM has a lower absorption coefficient than the FIR o-ray generated with FCPM.

We have also verified that the dual-frequency dye laser system, shown in Fig. 1, can be operated with flashlamp-pumped Rhodamine 6G dye laser, although the dye laser output of our system was insufficient to generate detectable FIR in the mixing experiment. However, a flashlamp-pumped dye laser system of 100 KW peak power and

1  $\mu$ s pulsewidth would yield the same FIR signal for each pulse as our laser-pumped system with 600 KW peak power and 30 nsec pulsewidth. Because a repetition rate greater than 1 pulse/sec is possible with such a dye laser, the dual-frequency single dye cell scheme described here should make a very useful source for FIR spectroscopy. Compared with the other FIR generation experiments using  $\text{CO}_2$  lasers,<sup>2,5-7</sup> this system has the advantages of a large continuously tunable FIR range and the use of room-temperature mixing crystals.

#### ACKNOWLEDGEMENT

This work was performed under the auspices of the U. S. Atomic Energy Commission.

Table I. Summary of the mixing experiments on five different crystals.

Crystals	Tunable Range	Power (Frequency Observed)
LiNbO <sub>3</sub>	20 to 127 cm <sup>-1</sup> (FCPM)	See Fig. 2
	20 to 95 cm <sup>-1</sup> (BCPM)	≈ twice that of FCPM
	40 to 160 cm <sup>-1</sup> (NCPM)	See Fig. 2
ZnO*	≤ 190 cm <sup>-1</sup> (FCPM)	14 mW (190 cm <sup>-1</sup> )
CdS*	≤ 180 cm <sup>-1</sup> (FCPM)	3 mW (180 cm <sup>-1</sup> )
ZnS*	≤ 91 cm <sup>-1</sup> (FCPM)	0.74 mW (91 cm <sup>-1</sup> )
CdSe*	≤ 150 cm <sup>-1</sup> (FCPM)	< 0.15 mW <sup>†</sup> (150 cm <sup>-1</sup> )

\* crystal thickness 1 mm

† less than the detector noise level

REFERENCES

1. D. H. Auston , A. M. Glass, and P. LeFur, Appl. Phys. Letters 23, 47 (1973).
2. R. L. Aggarwal, B. Lax, and G. Favrot, Appl. Phys. Letters 22, 329 (1973).
3. K. H. Yang, P. L. Richards, and Y. R. Shen, Appl. Phys. Letters 19, 320 (1971).
4. J. R. Morris and Y. R. Shen, Opt. Comm. 3, 81 (1971).
5. G. D. Boyd, T. J. Bridges, C. K. N. Patel, and E. Buehler, Appl. Phys. Letters 21, 553 (1972).
6. Van Tran Nguyen and T. J. Bridges, Phys. Rev. Letters 29, 359 (1972).
7. T. J. Bridges and A. R. Strnad, Appl. Phys. Letters 20, 382 (1972).
8. J. R. Morris or K. H. Yang, Ph.D. thesis 1973, Dept. of Physics, University of California, Berkeley (unpublished).
9. Notice that the scheme shown in Fig. 1 can be used to do the NCPM experiment if a GTP is placed right after the laser output mirror to separate the two beams.
10. Herschel S. Pilloff, Appl. Phys. Letters 21, 15 (1972). We independently developed this laser scheme.
11. For linewidth narrowing method, see for example, T. W. Hänsch, Appl. Opt. 11, 895 (1972).
12. See J. A. Armstrong, Appl. Phys. Letters 9, 72 (1966); for a similar scheme for sum frequency generation generation in transmission.
13. See, for example, C. H. Henry and C. G. B. Garrett, Phys. Rev. 171, 1058 (1968). Multi-polariton modes were included in our calculation. We used the oscillator strengths of A. S. Barker, Jr. and R. Loudon, Phys. Rev. 158, 433 (1967), and Raman cross section of I. P. Kaminow and W. D. Johnston, Jr., Phys. Rev. 160, 519 (1967).

14. D. R. Bosomworth, Appl. Phys. Letters 9, 330 (1966).
15. We were not able to deduce the absorption constant  $\alpha_3$  for the e-ray from the mixing experiment. The FIR e-ray signal generated with FCPM via  $\chi_{22}^{(2)}$  was too weak and the values of  $\alpha_3$  deduced from the NCPM results were rather inaccurate because of the 4-mrad laser divergence.
16. We used the optical refractive indices of G.D. Boyd. Robert C. Miller, K. Nassau, W. L. Bond, and A. Savage, Appl. Phys. Letters 5, 234 (1964).
17. A. Yariv, Quantum Electronics, (John Wiley, N.Y., 1967) p. 302.

FIGURE CAPTIONS

Fig. 1. One of the far-infrared generation setups. The wavelength of the two beams can be independently varied from 8100 Å to 8400 Å using a single dye cell.

Fig. 2. Far-infrared power generated vs frequency for two phase-matching conditions. The far-infrared power is **normalized** by a sum frequency power. The solid curves are the theoretical calculations based on data of the far-infrared absorption and the Raman cross-section in  $\text{LiNbO}_3$ . The insert shows the experimental geometry for non-collinear phase-matching which was achieved by a coupled translation and rotation of the prism.

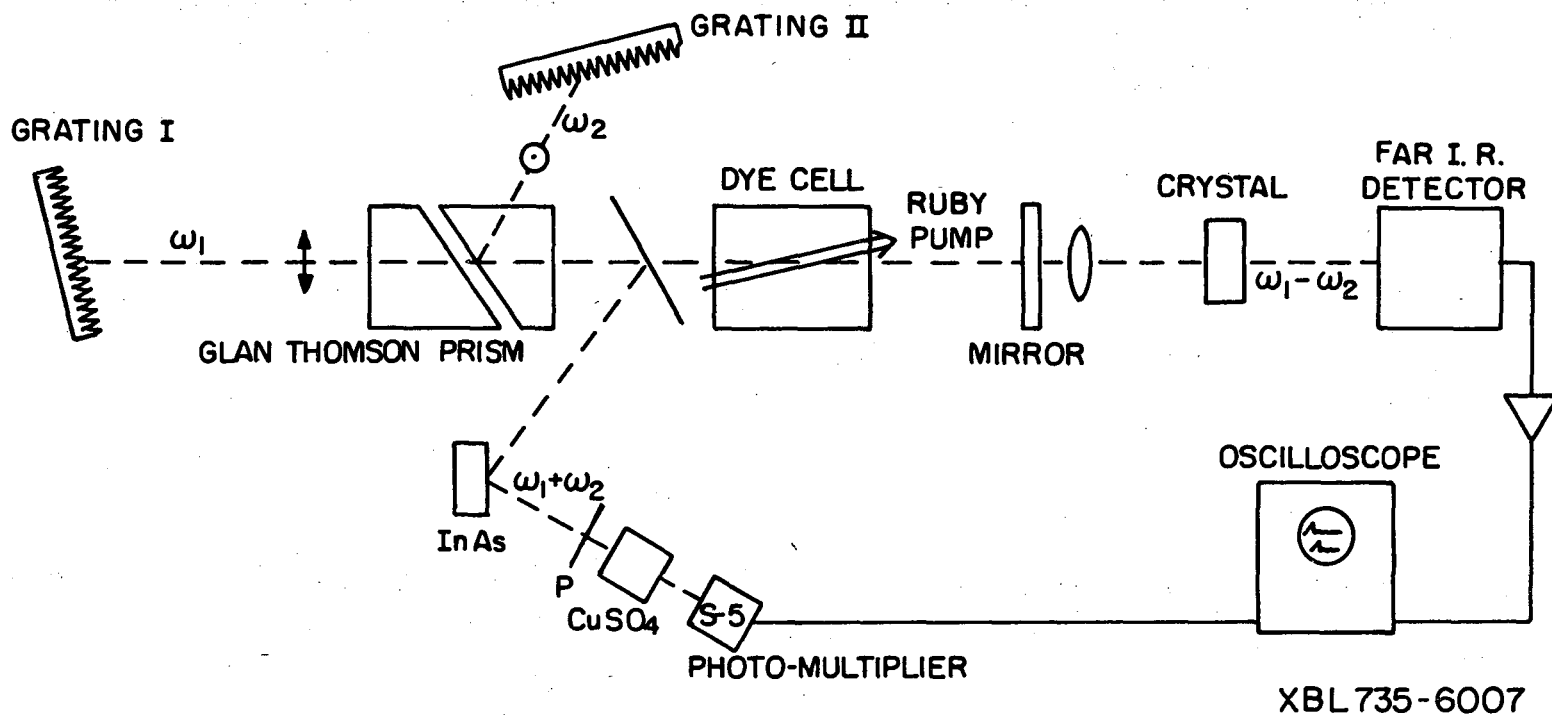
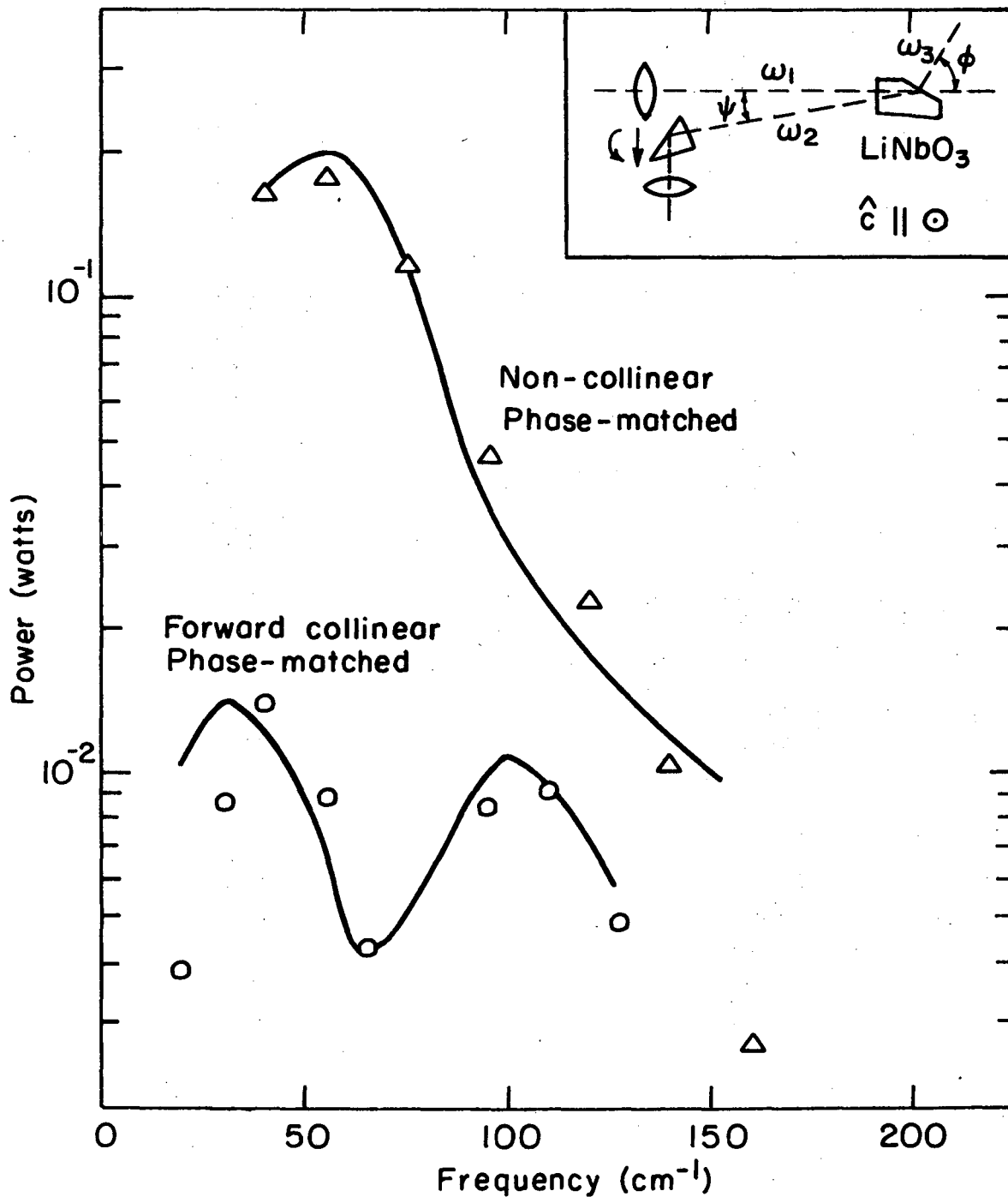


Fig. 1



XBL 738-1787

Fig. 2

LEGAL NOTICE

*This report was prepared as an account of work sponsored by the United States Government. Neither the United States nor the United States Atomic Energy Commission, nor any of their employees, nor any of their contractors, subcontractors, or their employees, makes any warranty, express or implied, or assumes any legal liability or responsibility for the accuracy, completeness or usefulness of any information, apparatus, product or process disclosed, or represents that its use would not infringe privately owned rights.*

TECHNICAL INFORMATION DIVISION  
LAWRENCE BERKELEY LABORATORY  
UNIVERSITY OF CALIFORNIA  
BERKELEY, CALIFORNIA 94720